

Analytical prediction of formed geometry in multi-stage single point incremental forming

R. Lingam · A. Bansal · N. V. Reddy

Received: 11 September 2014 / Accepted: 18 February 2015 / Published online: 15 March 2015
© Springer-Verlag France 2015

Abstract Single Point Incremental Forming (SPIF) is a die-less forming process that can be economically used for low volume production of sheet metal components. One of the limitations of SPIF is the maximum wall angle that can be formed in a single stage. To overcome this limitation, Multi-stage Single Point Incremental Forming (MSPIF) is used to form components with large wall angles. When the tool is moved from out-to-in during any stage, material present ahead of it (towards the centre of the component) moves down rigidly. If this rigid body displacement is not considered during tool path generation for MSPIF, it leads to stepped/unwanted features. Predicting the component geometry after each stage helps in monitoring the shape being developed and in turn is useful in designing intermediate stages to form required final geometry with desired accuracy. In the present work, a simple methodology is proposed to predict rigid body displacement based on tool path and process parameters (tool diameter, incremental depth, sheet thickness) used. Tool and sheet deflections due to forming force are also considered to predict final geometry of the component. Proposed methodology is validated by comparing predicted profiles with experimentally measured profiles of high wall angle axisymmetric components formed using different materials and sheet thicknesses. Predicted profiles are in good agreement with experimental results.

Keywords Incremental sheet metal forming · Rigid body displacement · Multi-stage forming

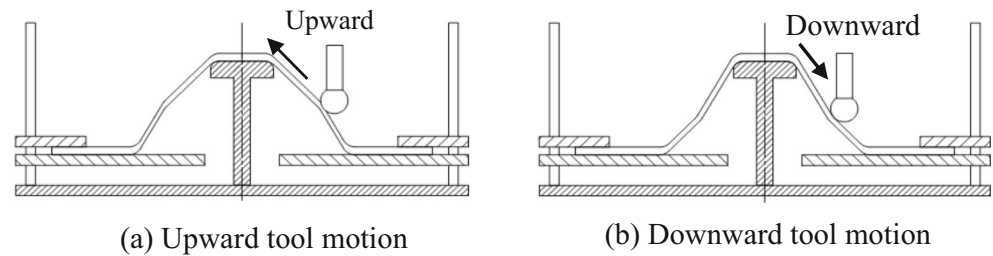
Introduction

Single Point Incremental Forming (SPIF) is a die-less forming process that uses a hemispherical or spherical ended moving tool to deform the sheet metal in a series of small deformations. High forming limits, low forming force and forming without component specific tooling make SPIF a competitive alternative to economically produce sheet metal components in low volume. There is a limitation on maximum angle that can be formed using single stage SPIF, hence multiple stages are preferred to form components with large wall angles [1]. More recently, Cao et al. [2] and Reddy et al. [3] presented a comprehensive review of the latest literature on incremental forming including Multi-stage Single Point Incremental Forming (MSPIF). They also presented a tool path generation methodology based on the geometry and surface finish requirements in incremental forming and finally demonstrated a new double-side incremental forming process to form parts with double curvatures on both sides of the initial plane of the sheet.

Generally formability in SPIF is represented by the maximum wall angle that can be formed without failure [1]. Single-stage SPIF can successfully form wall angles up to 60~70° for various aluminium as well as steel sheets of 1 mm initial thickness using suitable process parameters [1]. However, forming wall angles close to 90° using SPIF is difficult. There are few attempts to form high wall angle components using MSPIF [4–9]. Hirt et al. [4] proposed a multi-stage strategy to form asymmetric geometries using the Two Point Incremental Forming (TPIF). In this strategy the sheet is pre-formed to a shallow wall angle using downward motion of the tool which is followed by number of stages of alternating upward and downward tool motion as shown in Fig. 1. They have successfully formed truncated pyramids with wall angles up to 80°. Here note that the material from outside the component opening is shifted to the component wall region. Duflou et al. [5]

R. Lingam · A. Bansal · N. V. Reddy (✉)
Department of Mechanical and Aerospace Engineering, Indian
Institute of Technology Hyderabad, Hyderabad, India
e-mail: nvr@iith.ac.in

Fig. 1 Multi-stage forming strategy using TPIF [4]



formed conical components having large wall angle using five stages as shown in Fig. 2a. They formed the horizontal region of work-piece at the centre of component that does not get deformed during single stage forming of high wall angle component. Here the tool is always moved from the outer periphery towards the centre of the sheet. Note that there is no support at the centre of the component as in [4].

Skjoedt et al. [6] proposed a five stage tool path (Fig. 2b) to form a cylindrical cup with 90° wall angle and height to diameter ratio as unity. They used two strategies, namely, Down-Down-Down-Up (DDDU) and Down-Up-Down-Down (DUDD) in which the tool moved to the desired final component depth in all stages. In DUDD strategy component failed during 4th stage, whereas in DDDU strategy, it successfully formed up to 4th stage. Note that the formed component had an unwanted cone at the centre of component which can be attributed to the rigid body displacement during Down (D) passes. In addition, they demonstrated that the thickness variation is not only dependent on the tool path used, but also on its direction (downwards or upwards) in each stage. Skjoedt et al. [7] modified their tool path of [6] and used DDDU strategy to successfully form a cylindrical cup with 90° wall angle. In the first stage they formed the component to a depth less than the required one and gradually increased the wall angle and depth in subsequent stages. They reported high thickness strains in the transition zone from vertical wall to horizontal base, where bi-axial stretching takes place. Abhishek [8] and Malhotra et al. [9] proposed the use of both in-to-out and out-to-in tool paths within a stage (Fig. 2c) to

shift the material from both wall and base regions to corner of cylindrical component and have successfully formed a 90° wall angle cylindrical component with near flat base.

Kim and Yang [10] compared two strategies with double passes to form high wall angle components using SPIF. In the first strategy intermediate geometry is obtained by linearly blending initial and final geometry of the sheet. In the second strategy intermediate geometry is calculated such that the regions requiring severe deformation in final shape are subjected to less deformation in intermediate shape. They concluded that the second strategy resulted in higher formability, better thickness distribution and higher mechanical strength of the formed component. Young and Jeswiet [11] experimentally studied the effect of single-pass and double-pass forming strategies on the thickness distribution while forming a cone with 70° wall angle. They concluded that double-pass strategy resulted in uniform thinning. In addition, they concluded that the sine law over predicts the thicknesses beyond wall angles of 40° .

Tool movement from out-to-in as shown in Fig. 3 causes rigid body displacement of the material present ahead of it (towards the centre of the component). This aspect was not considered in the earlier attempts [5–7] while deciding the intermediate profiles in MSPIF. Hence, the depths as well as the geometry of formed components differed from the desired ones. It is very important to predict the geometry of component after each stage to design the subsequent stages. Malhotra et al. [9] have developed a model to predict the rigid body displacement based on the theory of large elastic deflection of

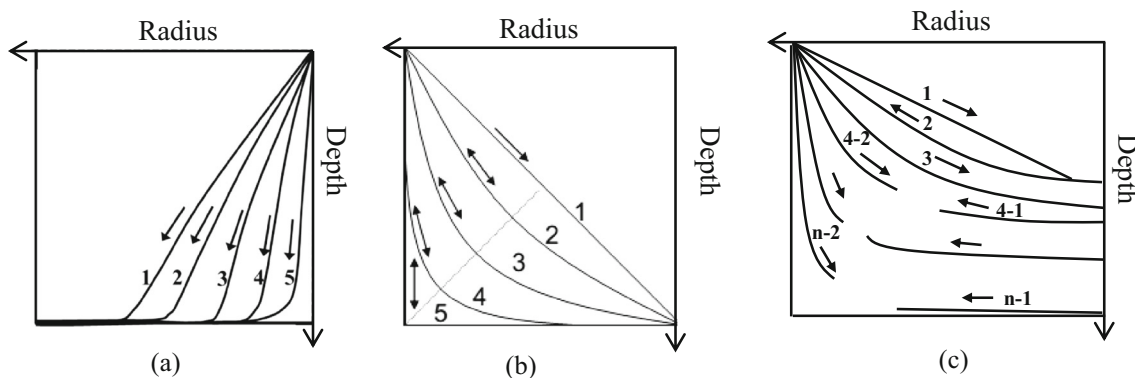


Fig. 2 Multi-stage strategies for forming cup (a) Dufflou et al. [5] (b) Skjoedt et al. [6, 7] (c) Abhishek [8] and Malhotra et al. [9]

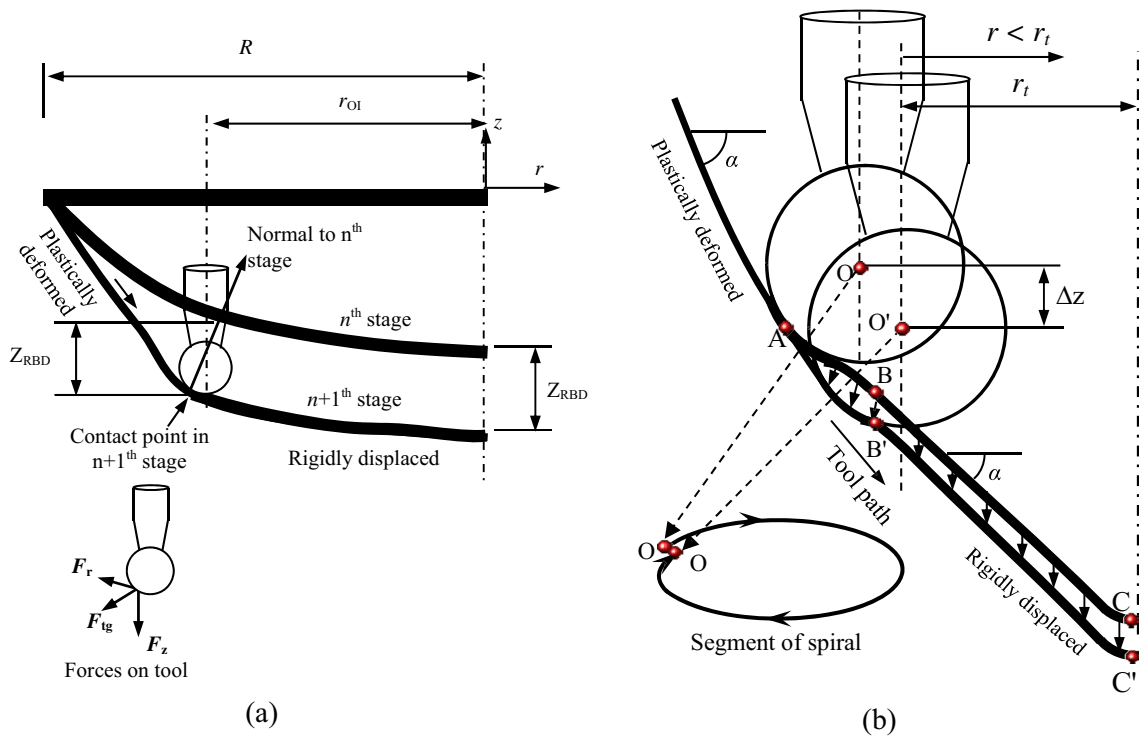


Fig. 3 Rigid body displacement during OI tool path

beams [12]. Their model requires calibration of three constants (γ , a , b) using FEA simulations for each material and thickness of sheet used during forming. To reduce the number of finite element simulations needed in their methodology, Xu et al. [13] assumed that the three constants (γ , a , b) vary linearly with yield strength (σ_y) of the material and initial sheet thickness (t_0). They related the constants (γ , a , b) to yield strength and sheet thickness using three coefficients (λ , ρ , χ) which are obtained by carrying out six FEA simulations. They used SS304, Ti6Al4V of different thicknesses to carry out FEA simulations during calibration.

In the present work a simple methodology is proposed to predict the formed geometry after each stage in MSPIF. Rigid body displacement at any instant of forming is dependent only on the tool path used without considering elastic recovery that takes place during incremental sheet metal forming. The final geometry after each stage is also affected by the elastic deflections of tool and sheet which get recovered. In the proposed methodology, both these aspects are considered to predict the component geometry after each stage. Tool and sheet deflections are calculated using thickness distribution and force prediction methodologies published earlier [14, 15].

Methodology

In multi-stage forming, the final geometry is formed in several stages and an intermediate geometry is formed after each

stage. Tool can be moved either out-to-in or in-to-out in each stage. In out-to-in tool path (here after called “OI tool path”), tool starts close to the clamped boundary (radius R) and moves towards centre while moving down in z direction (Fig. 3a). Fig. 3a shows that the tool started deforming the sheet from radius R and moved up to radius r_{OI} during $n+1^{th}$ stage. It can also be clearly noticed from Fig. 3a that the thickness in the region deformed during $n+1^{th}$ stage is less than the thickness after n^{th} stage. Material present ahead of the tool (from r_{OI} to centre) rigidly moves down as shown in Fig. 3a. It can be realized that rigid body displacement without considering elastic deflections of forming tool and sheet due to forming

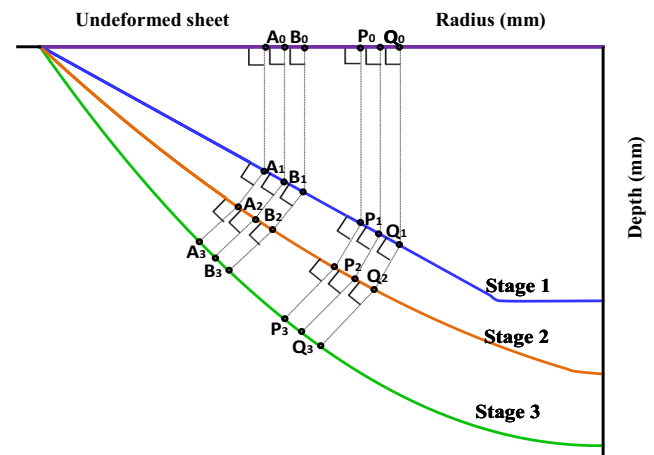


Fig. 4 Schematic illustration of material movement to calculate sheet thickness during multi-stage forming [8]

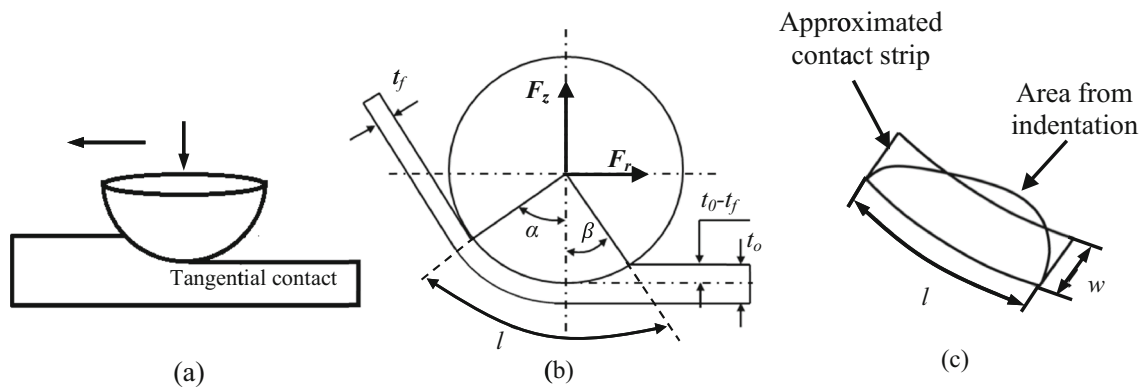


Fig. 5 Contact area and forming force prediction

forces can be easily predicted using down word movement of tool from starting location to current location. It is also clearly known from literature [1, 3, 14] that tool and sheet get elastically deflected and the same has to be considered for accurate prediction of rigid body displacement and formed geometry after each stage.

Schematic representation of material movement along the cross sectional profile of a component during tool movement along a segment of spiral path is shown in Fig. 3b. During this movement the tool moved down by Δz from O to O'. The material present in region AB (Fig. 3b) during n^{th} stage is deformed to AB' in $n+1$ th stage. Material present in region BC ($r < r_i$) in n^{th} stage rigidly moved to B'C' maintaining tangency with tool at B' (Fig. 3b). Note that the rigid body displacement throughout BC is equal (i.e., $BB'=CC'$). Rigid body displacement gets accumulated throughout OI tool path. Let this accumulated rigid body displacement be Z_{RBD} after completion of OI path in a given stage (i.e., when the tool reaches to r_{OI} (Fig. 3a)). Assuming that the material which comes in contact with tool at any instant moves normal to n^{th} stage during $n+1$ th stage, Z_{RBD} can be estimated as the z-distance between the contact point at r_{OI} and its normal projection on to n^{th} stage (Fig. 3a). If Z_{OI}^n is the z location of a point on the component after n^{th} stage and Z_{OI}^{n+1} is the z location o that point on the formed

component after OI tool path of $n+1$ th stage, then Z_{OI}^{n+1} can be expressed as:

$$Z_{OI}^{n+1} = \begin{cases} Z_{OI}^n + Z_{RBD} & 0 \leq r < r_{OI} \text{ (undeformed region)} \\ Z_{OI}^n + f(\Delta z) & r_{OI} \leq r \leq R \text{ (deformed region)} \end{cases} \quad (1)$$

where, $Z_{OI}^n + f(\Delta z)$ is the Z location of contact point during OI tool path in $n+1$ th stage.

Elastic deflections of sheet and tool which gets recovered can be estimated accurately by predicting forming force at any instant. To predict forming force with good accuracy, thickness distribution of formed force component is obtained by assuming plane-strain deformation and volume constancy. Then the stress components are obtained assuming plane strain deformation and yielding according to von-Mises yield criterion. Note that thickness, meridional and circumference directions are assumed to be the principal stress directions. Force components along thickness (t), meridional (ϕ) and tangential (θ) direction are then obtained by assuming that the stress components are uniformly distributed throughout contact zone [14, 16].

To calculate the thickness, first initial sheet configuration is divided into several small elements of equal length. Thickness of each element after first stage is calculated considering overlap in deformation zone [15]. From second stage onwards, it is

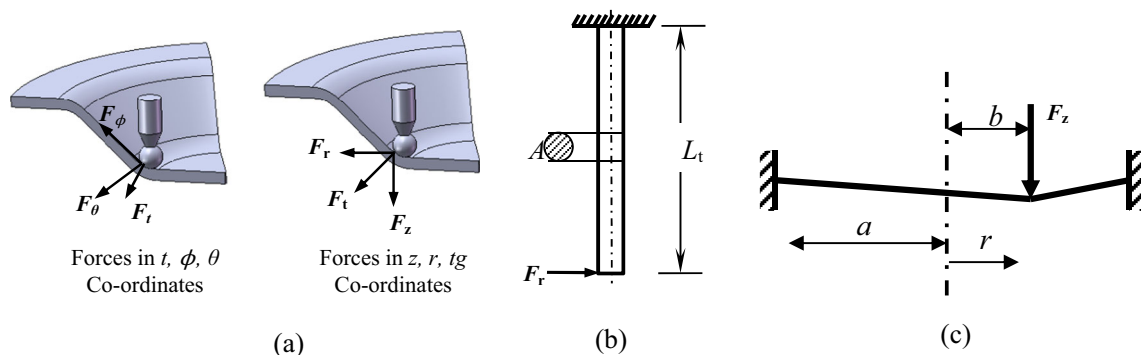
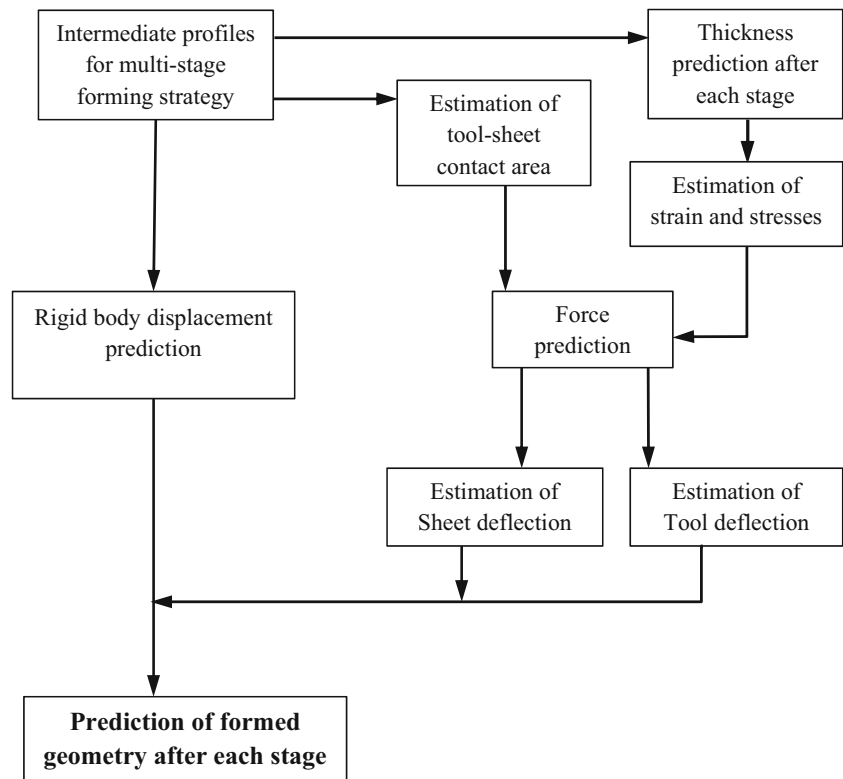


Fig. 6 Tool and sheet deflection due to forming force

Fig. 7 Flowchart chart representing the steps in predicting the formed geometry



assumed that the material moves normal to n^{th} stage profile during $n+1$ th stage as shown in Fig. 4 and the thickness is calculated by applying volume constancy element by element [8]. Equivalent strain (ϵ_{eq}) is estimated considering the deformation to be plane strain satisfying von-Mises yield criterion. Equivalent stress (σ_{eq}) is estimated using the stress–strain relation of the sheet material being deformed. Stress components in thickness (σ_t), meridional (σ_ϕ) and circumferential (σ_θ) directions are calculated using the following expressions [15, 16]:

$$\sigma_t = -\frac{2\sigma_{eq}}{\sqrt{3}} \left(\frac{t}{R_t + t} \right) \sigma_\phi = \frac{2\sigma_{eq}}{\sqrt{3}} \left(\frac{R_t}{R_t + t} \right) \sigma_\theta = \frac{\sigma_{eq}}{\sqrt{3}} \left(\frac{R_t - t}{R_t + t} \right) \quad (2)$$

where R_t is the radius of tool and t is the instantaneous thickness of the sheet.

To calculate the contact area, tool motion is approximated as indentation followed by sliding [14, 17]. Tool is assumed to leave contact with the sheet tangentially along the

circumferential direction as shown in Fig. 5a. Hence the area of contact in incremental forming is estimated as half the area of indentation of a spherical ball in to a flat base with an inclined wall (inclination equal to wall angle) during the first stage. Area of contact is approximated as a rectangle (Fig. 5c) based on the contact pressure observed during FEA [14, 18]. Length of rectangle (l) is taken as the contact length along meridional direction ($l = R_t (\alpha + \beta)$, where α is the wall angle and β is the groove angle as shown in Fig. 5b). Contact area for second to final stages is estimated considering the tool contact condition shown in Fig. 3b. The width of rectangle (w) is calculated by equating the area of rectangle to the estimated contact area. Force components (F_t, F_ϕ, F_θ) are calculated by assuming that the stress components ($\sigma_t, \sigma_\phi, \sigma_\theta$) are uniformly distributed over the deformation zone. Force components (F_t, F_ϕ, F_θ) are then resolved to find the components along axial (F_z), radial (F_r) and tangential (F_{tg}) directions (Fig. 6a).

Radial force (F_r) causes the forming tool to deflect towards the centre of component and force along the axis of tool (F_z) causes the sheet to deflect in z direction which gets regained.

Table 1 Comparison of axial force (F_z) predictions with Aerens et al. [18] for cone with 50° formed using Al 8011 and Al 5052

Material	Thickness (mm)	Axial force (N) present methodology	Axial force (N) Aerens et al. [18]	% deviation
8011	1.5	925	884	4.6
8011	1.0	430	468	–8.1
5052	1.0	750	798	–6

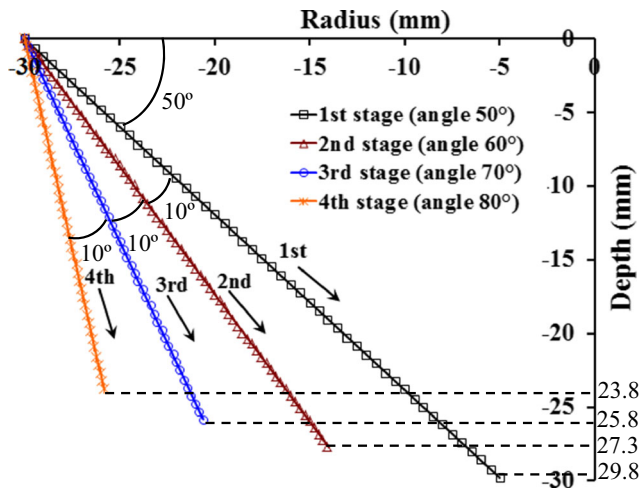


Fig. 8 Four stage tool path to form 80° wall angle component

Assuming the tool as cantilever beam of length L_t with force (F_r) acting at its free end (Fig. 6b), the deflection of tool (δ_{tool}) at the contact point is estimated as:

$$\delta_{tool} = \frac{F_r L_t^3}{3EI} \tag{3}$$

where E is the Young’s modulus of tool material, I is the moment of inertia. Although the tool geometry deviates from cylindrical geometry near the tool tip, it is assumed as a regular cylinder to calculate moment of inertia ($I = \pi d_s^4 / 64$) where d_s is the diameter of the tool shank.

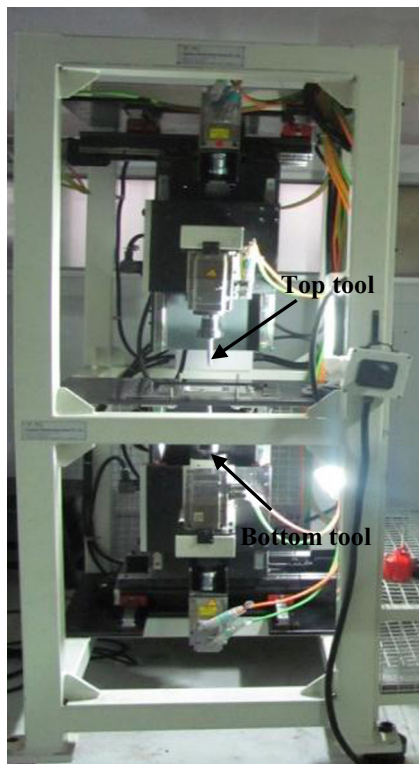


Fig. 9 Custom built Double Sided Incremental forming machine

Table 2 Axial forces predicted using present methodology

	Al 8011, 1.5 mm		Al 8011, 1.0 mm		Al 5052, 1.0 mm	
	F_z (N)	F_r (N)	F_z (N)	F_r (N)	F_z (N)	F_r (N)
Stage 1	855	311	418	127	690	232
Stage 2	403	172	167	69	292	126
Stage 3	380	165	141	65	251	120
Stage 4	340	139	135	54	234	99

The sheet deflection is schematically shown in Fig. 6c and can be estimated using the expression developed by Timoshenko [19]:

$$\delta_{sheet} = \frac{F_z}{8\pi D} \left[-(r^2 + b^2) \ln\left(\frac{a}{b}\right) + (r^2 - b^2) + \frac{1}{2} \left(1 + \frac{b^2}{a^2} \right) (a^2 - r^2) \right] \tag{4a}$$

$$D = E_s t^3 / 12(1 - \nu^2) \tag{4b}$$

where F_z is the axial force, a is half of the opening length of fixture, b is the distance of applied force from the centre of sheet, r is the distance of the point at which deflection is calculated from the centre of the sheet, E_s is Young’s modulus of sheet material, t is sheet thickness and ν is Poisson’s ratio.

The procedure followed to predict the component geometry after each stage using proposed methodology is presented as a flow chart in Fig. 7.

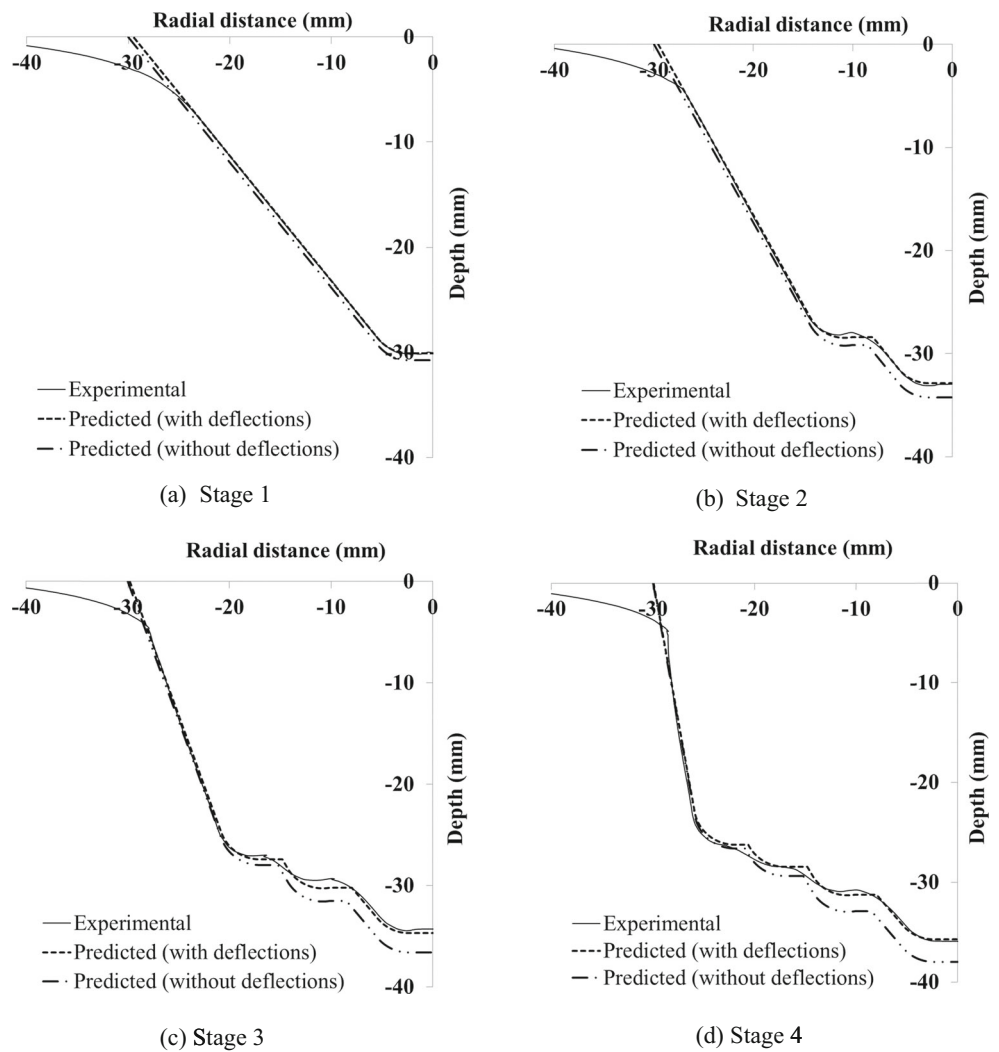
Results and discussion

Methodology presented in section 2 is implemented for axisymmetric components. Force predictions of implemented methodology is validated with the experimental values reported by Aerens et al. [18] as the accuracy of force prediction is important to estimate elastic deflections of tool as well as sheet during incremental forming. They [18] have carried out parametric study of forces measured by forming cones of various angles (α) using different materials, sheet thicknesses (t), tool diameters (D) and incremental depths (Δz) and obtained a generalized regression equation for force along the axis of tool (F_z) as:

$$F_z = 0.0716 R_m t^{1.57} D^{0.41} \Delta h^{0.09} \alpha \cos \alpha \tag{5}$$

where R_m is the tensile strength and Δh is the scallop height given by $\Delta h = \frac{\Delta z^2}{4(\sin \alpha)^2} D$. Note that the above expression is used to validate predictions of force equilibrium method presented in section 2, using the parameters within the range of values used to obtain the same. In addition, comparison of axial force predictions (F_z) for first stage is appropriate, as

Fig. 10 Comparison of measured and predicted profiles after each stage of component formed using Al 8011, 1.5 mm thick sheet



the above expression is developed for single stage. Two materials used in the present study are Al 8011 (Tensile strength 119 MPa, flow curve $\sigma=117\varepsilon^{0.032}$) and Al 5052 (Tensile strength 203 MPa, flow curve $\sigma=332\varepsilon^{0.12}$) and the same are

used for the validation of force predictions. Other process parameters used for the results presented in Table 1 are incremental depth (Δz) of 0.5 mm, tool diameter (D) of 10 mm (not same as that used to form components), wall angle (α) of 50° .

Fig. 11 Comparison of predicted and measured profiles after 4th stage of the components formed using Al 8011, 1 mm thickness and Al 5052, 1 mm thickness sheets

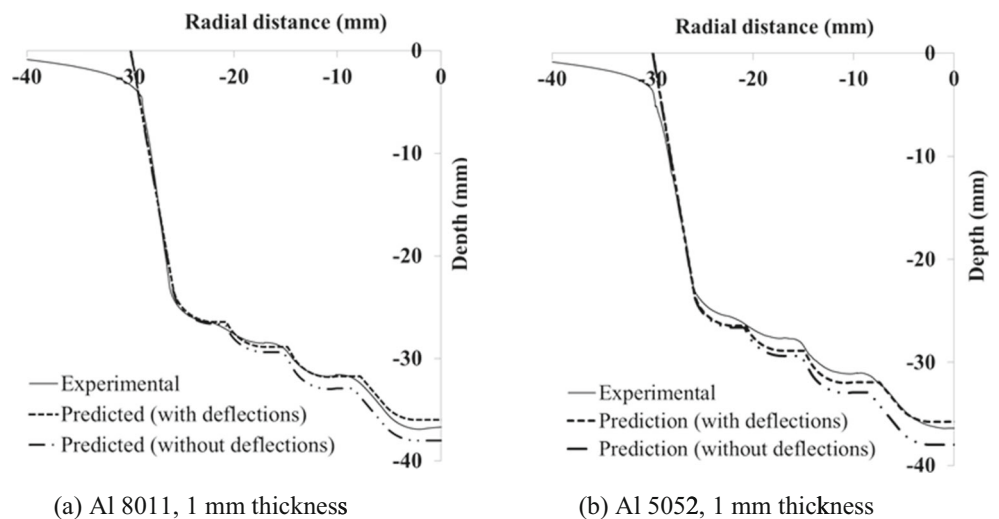


Fig. 12 Comparison of profiles predicted by present methodology with that of Malhotra et al. [9]

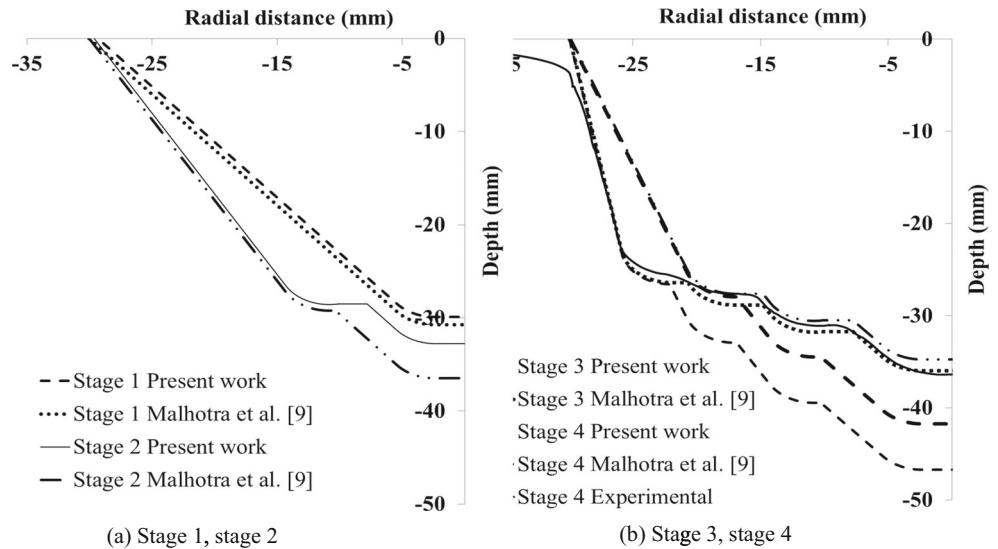


Table 1 shows the comparison between the force prediction using present methodology and the predictions of expression developed by Aerens et al. [18]. Results presented in Table 1 show that the predictions of present methodology are in good agreement with that of predicted using the expression developed by Aerens et al. [18]. Note that the predictions of force equilibrium method are for assumed principal stress directions whereas those of Aerens et al. [18] are based on experiments.

Experiments as well as predictions are carried out using two materials (Al 8011 and Al 5052) and two thicknesses of one of those materials (Al 8011–1.5 mm thickness, Al 8011–1 mm thickness) to demonstrate the predictive capabilities of

present methodology. Component geometry used during the present work is similar to that of used by Duflou et al. [5]. Predictions as well as experiments are carried out to form an 80° wall angle component (Fig. 8) in four stages starting with 50° wall angle in the first stage and an increase of 10° wall angle in subsequent three stages. Experiments are carried out on a custom built double sided incremental forming machine using only top tool (Fig. 9). A fixture with 100 × 100 mm work area is used to mount the sheet on the machine. Incremental depth (Δz) of 0.5 mm and tool diameter (D) of 8 mm are used during all stages. Length of forming tool (L_t) used is 65 mm and its shank diameter (d_s) is 13 mm. Spiral tool path is used to form the components. Forming forces predicted by force equilibrium methodology which is used in present work during each stage are presented in Table 2.

Figure 10 shows the comparison of predicted profiles in four stages with and without considering elastic deflections of tool and sheet with that of measured geometry after unclamping the component from fixture. Material used for predictions is Al 8011 with 1.5 mm thickness. Predicted profiles after each stage without considering deflections are obtained by shifting down the material ahead of the tool towards centre of sheet by a distance equal to rigid body displacement predicted for that stage (3.85, 2.62 and 1.44 mm for 2nd, 3rd and 4th stages respectively). It can be seen from Fig. 10 that profiles predicted without considering sheet and tool deflections lie outside the measured profile in all stages. Elastic deflections of tool and sheet at any instant during deformation are estimated using Eqs. (3) and (4a). It can be clearly seen from the above figure that the predicted profiles are in good agreement with that of measured profiles after considering the recovery of elastic deflections of sheet and tool ((sheet - 0.58 mm, tool - 0.09 mm), (sheet - 0.45 mm, tool - 0.05 mm), (sheet - 0.22 mm, tool - 0.05 mm) and (sheet - 0.15 mm, tool - 0.04 mm) during 1st, 2nd, 3rd and 4th stages respectively). The deviation of

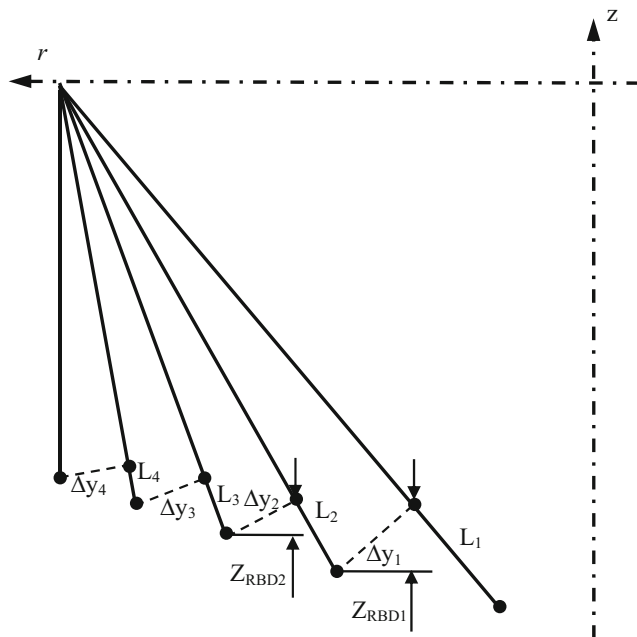
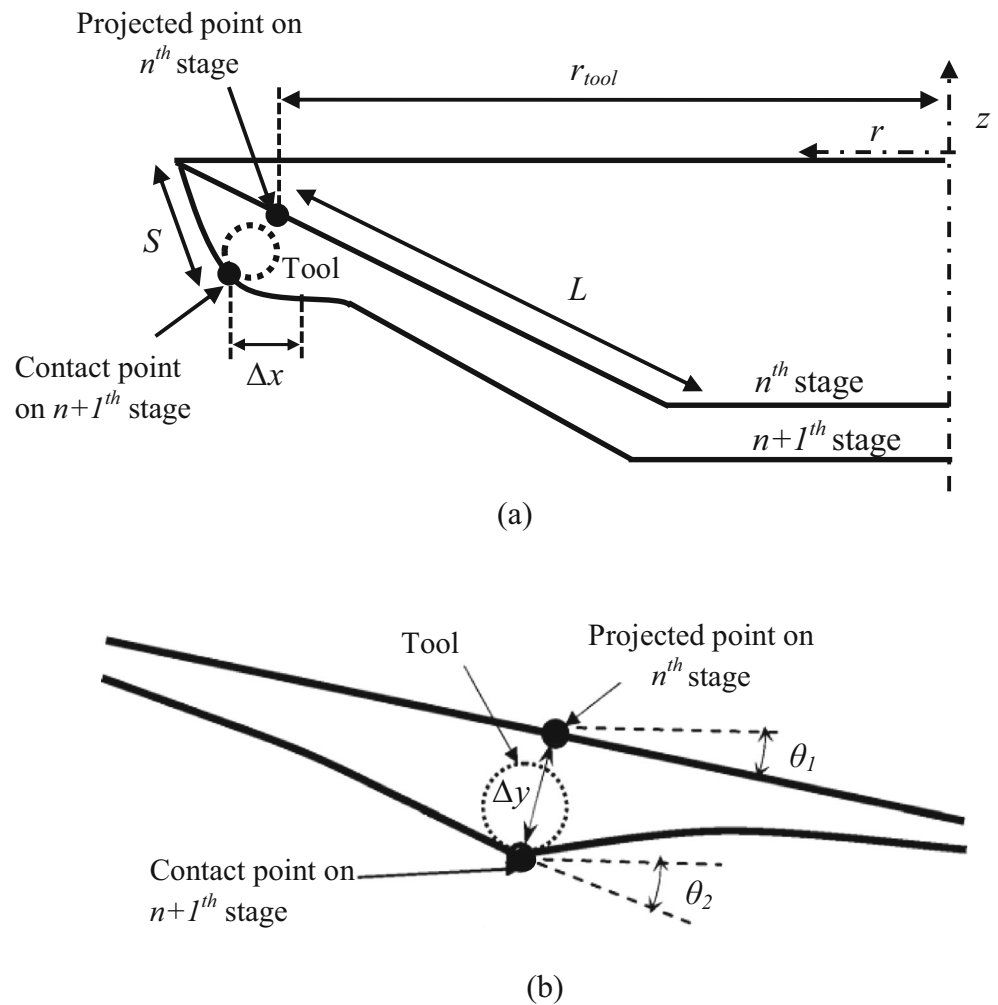


Fig. 13 Prediction of rigid body displacement by Malhotra et al. [9] methodology for complete OI tool paths

Fig. 14 Prediction of rigid body displacement by Malhotra et al. [9]



predicted depth with that of measured at centre of component without and with considering elastic recovery are (0.61, 0.06 mm), (1.4, 0.1 mm), (1.9, 0.38 mm) and (2.3, 0.2 mm) after 1st, 2nd, 3rd and 4th stages respectively.

Predicted profiles of present work without considering elastic deflections of sheet and tool remains same as they are only dependent on the downward movement of the tool from starting location to the current location as discussed earlier. Elastic deflections of sheet and tool are dependent on material properties as well as process conditions. Experiments as well as predictions are carried out by changing sheet thickness (Al8081, 1 mm) and material (Al5052, 1 mm) with and without considering elastic deflections of sheet and forming tool and their comparison after 4th stage is presented in Fig. 11. Note that the predicted profile (Fig. 11) without considering elastic recovery of sheet and tool is same as that shown in Fig. 10. It can be seen from Fig. 11 that the predicted profiles after considering elastic deflections of tool and sheet are in good agreement with the measured profiles (error in depth is 0.9 mm for Al 8011 and 0.6 mm for Al 5052). From the results presented in this section, one can conclude that the deviation of formed

profile for different materials and process parameters is due to tool and sheet deflection caused by forming forces.

Comparison of profiles predicted using present methodology with that of FEA based calibration methodology (explained in appendix A) [9, 13] for component formed using Al 5052 with 1 mm thick sheet is shown in Fig. 12. While implementing their methodology [9, 13], it is realized that the elliptic integrals given by Xu et al. [13] are not in correct order. However, it is rectified by taking correct sequence form Yu and Zhang [12] for generating the results for comparison. Malhotra et al. [9] used implicit FEA analysis with shell elements to obtain the constants ($\gamma=5.0$, $a=1.0$, $b=4.0$) for Al 5052 sheet with 1 mm thickness. Xu et al. [13] used SS304 and Ti6Al4V for calibration hence their results are not compared during present work. It can be seen from Fig. 12 that their methodology [9] over predicts rigid body displacement after each stage. The reason for over prediction is explained with the help of Fig. 13. The rigid body displacement in OI tool path using FEA based methodology [9] can be rewritten as (details are given in appendix A):

$$Z_{RBD-OI} = \Delta y - L * f(\theta_1, \theta_2, S) \quad (6)$$

where θ_1, θ_2 are wall angles as shown in Fig. 14b and S is the distance from component opening to the contact point along $n+1$ th profile (Fig. 14b). Both θ_1, θ_2 are constant along the profile for constant wall angle geometries like the ones used in present work. The value of Δy increases and L decreases proportionately with z -motion of tool. Further the value of $f(\theta_1, \theta_2, S)$ estimated for each stage is below 0.01. Hence, the effect of L^*f in equation 6 is negligible. Finally Z_{RBD-OI} is approximately represented by Δy which is the normal distance between contact point in $n+1$ th stage and its projection on n^{th} stage profile (Figs. 13 and 14b). This shows that their methodology depends on both sheet material and component geometry. In addition, it is realized that the prediction of rigid body displacement using the methodology developed by Malhotra et al. [9] is in opposite direction than correct direction up to certain depth from the initial plane of the sheet.

Conclusions

Multi-stage incremental forming can be used to form components with wall angles beyond single stage formability limit. However, the rigid body displacement in each stage results in deviation of the formed component from the desired geometry. A simple methodology is presented in this work to predict the geometry of formed components using OI tool path and incremental forming process parameters. Results presented indicate that the rigid body displacement is dependent on the tool path used and the variation in profiles of components formed using different materials and sheet thicknesses is due to the tool and sheet deflections caused by forces acting on them. Further work is in progress to predict profiles of free form components as well as designing intermediate stages to form desired geometries with required thickness distribution.

Appendix A. Rigid body displacement prediction proposed by Malhotra et al. [9] and Xu et al. [13]

In this model the rigid body displacement for OI pass is given by:

$$Z_{RBD-OI} = \Delta y - \left(\frac{L}{\gamma}\right) \left(1 - \frac{2[E(R) - E(\varphi_0, R)]}{K(R) - F(\varphi_0, R)}\right) \quad (7)$$

where Δy is the distance between contact point in $n+1$ th stage and its projection on to the profile after n^{th} stage (Fig. 14b), L is the length of profile in n^{th} stage from the projected point to the base (Fig. 14a), γ is a constant calibrated using FEA, $K(R)$, $E(R)$ are the complete elliptic integrals of first and second kind respectively and $F(\varphi_0, R)$, $E(\varphi_0, R)$ are the incomplete elliptic integrals of first and second kind respectively, φ_0, R are

the functions of θ_1, θ_2, S where θ_2 is the wall angle at the contact point in $n+1$ th stage, θ_1 is the wall angle at the projection of contact point on to the n^{th} stage profile (Fig. 14b) and S is the distance from component opening to the contact point along $n+1$ th profile (Fig. 14b).

References

- Jeswiet J, Micari F, Hirt G, Bramley A, Dufflou A, Allwood J (2005) Asymmetric single point incremental forming of sheet metal. *CIRP Ann Manuf Technol* 54(2):623–649
- Cao J, Huang Y, Reddy NV, Malhotra R, Wang Y (2008) Incremental sheet metal forming: advances and challenges. *Proceedings of 9th ICTP*: pp. 751
- Reddy NV, Lingam R, Cao J (2014) Incremental sheet metal forming processes. In *Nee AYC (ed) Handbook of manufacturing engineering and technology*, Springer
- Hirt G, Ames J, Bambach M, Kopp R (2004) Forming strategies and process modeling for CNC incremental sheet forming. *CIRP Ann Manuf Technol* 53(1):203–206
- Dufflou JR, Verbert J, Belkassam B, Gu J, Sol H, Henrard C, Habraken AM (2008) Process window enhancement for single point incremental forming through multi-step toolpaths. *CIRP Ann Manuf Technol* 57(1):253–256
- Skjoedt M, Bay N, Endelt B, Ingarao G (2008) Multi stage strategies for single point incremental forming of a cup. *Int J Mater Form* 1(1): 1199–1202
- Skjoedt M, Silva MB, Martins PFA, Bay N (2010) Strategies and limits in multi-stage single point incremental forming. *J Strain Anal Eng Des* 45(1):33–44
- Abhishek K (2009) Multi-stage tool path strategies for single point incremental forming. M.Tech thesis, Indian Institute of Technology Kanpur
- Malhotra R, Bhattacharya A, Kumar A, Reddy NV, Cao J (2011) A new methodology for multi-pass single point incremental forming with mixed tool paths. *CIRP Ann Manuf Technol* 60(1):323–326
- Kim TJ, Yang DY (2000) Improvement of formability for the incremental sheet metal forming process. *J Mech Sci* 42(7):1271–1286
- Young D, Jeswiet J (2004) Wall thickness variations in single-point incremental forming. *Proc Inst Mech Eng B J Eng Manuf* 218(11): 1453–1459
- Yu TX, Zhang LC (1996) *Plastic bending: theory and applications*. World scientific
- Xu D, Malhotra R, Reddy NV, Chen J, Cao J (2012) Analytical prediction of stepped feature generation in multi-pass single point incremental forming. *J Manuf Process* 14(4):487–494
- Asghar J, Lingam R, Shibin E, Reddy NV (2014) Tool path design for enhancement of accuracy in single-point incremental forming. *Proc Inst Mech Eng B J Eng Manuf* 228(9):1027–1035
- Bhattacharya A, Maneesh K, Reddy NV, Cao J (2011) Formability and surface finish studies in single point incremental forming. *J Manuf Sci Eng* 133(6):061020
- Silva MB, Skjoedt M, Atkins AG, Bay N, Martins PAF (2008) Single-point incremental forming and formability-failure diagrams. *J Strain Anal Eng Des* 43(1):15–35
- Adams D, Jeswiet J (2014) A new model for contact geometry in single-point incremental forming. *Proc Inst Mech Eng B J Eng Manuf*. doi:10.1177/0954405414535580
- Aerens R, Eyckens P, Van Vael A, Dufflou A (2010) Force prediction for single point incremental forming deduced from experimental and FEM observations. *Int J Adv Manuf Technol* 46(9–12):969–982
- Timoshenko S (1964) *Theory of plates and shells*, 2nd edn. McGraw-Hill, New York